Cerebral Cortex January 2012;22:144–157
doi:10.1093/cercor/bhr097
Advance Access publication May 30, 2011

Early Postnatal Migration and Development of Layer II Pyramidal Neurons in the Rodent Cingulate/Retrosplenial Cortex

Eloisa Zgraggen[1], Michael Boitard[1], Inge Roman[1], Michiko Kanemitsu[1], Gael Potter[1], Patrick Salmon[1], Laszlo Vutskits[1,2], Alexandre G. Dayer[1,3] and Jozsef Z. Kiss[1]

[1]Department of Neurosciences, University of Geneva Medical School, CH-1211 Geneva 4, Switzerl and [2]Department of Anesthesiology, Pharmacology and Intensive Care, University Hospital of Geneva, CH-1211 Geneva 4, Switzerland and [3]Department of Mental Health and General Psychiatry, University Hospital of Geneva, CH-1211 Geneva 14, Switzerland

Address correspondence to Prof. Jozsef Zoltan Kiss, MD, Department of Fundamental Neurosciences, University of Geneva Medical School, Rue Michel-Servet 1, CH-1211 Geneva 4, Switzerland. Email: jozsef.Kiss@unige.ch.

The cingulate and retrosplenial regions are major components of the dorsomedial (dm) limbic cortex and have been implicated in a range of cognitive functions such as emotion, attention, and spatial memory. While the structure and connectivity of these cortices are well characterized, little is known about their development. Notably, the timing and mode of migration that govern the appropriate positioning of late-born neurons remain unknown. Here, we analyzed migratory events during the early postnatal period from ventricular/subventricular zone (VZ/SVZ) to the cerebral cortex by transducing neuronal precursors in the VZ/SVZ of newborn rats/mice with Tomato/green fluorescent protein–encoding lentivectors. We have identified a pool of postmitotic pyramidal precursors in the dm part of the neonatal VZ/SVZ that migrate into the medial limbic cortex during the first postnatal week. Time-lapse imaging demonstrates that these cells migrate on radial glial fibers by locomotion and display morphological and behavioral changes as they travel through the white matter and enter into the cortical gray matter. In the granular retrosplenial cortex, these cells give rise to a Satb2+ pyramidal subtype and develop dendritic bundles in layer I. Our observations provide the first insight into the patterns and dynamics of cell migration into the medial limbic cortex.

Keywords: corticogenesis, dendritic bundles, lentivectors, medial limbic cortex, subventricular zone

Introduction

Linking the hippocampal formation and the amygdaloid complex to neocortical areas is central for sensory processing, memory, and motor responses. The cingulate cortex (CGC) and retrosplenial cortex (RSC) occupy a critical position in this communication. These regions have reciprocal connections with the anterior and dorsomedial (dm) thalamic nuclei, the hippocampal formation, the amygdaloid complex, and widespread neocortical areas (see review in Vogt 2005; Vogt and Laureys 2005; Vann et al. 2009). In primates, the cingulate gyrus can be subdivided into perigenual anterior CGC, midcingulate cortex, posterior CGC, and RSC (Vogt and Laureys 2005). Human functional neuroimaging studies, electrical stimulation, and stroke analyses provided evidence for a role of the anterior and midcingulate area in motivation, autonomic regulation, emotional regulation, and motor responses, while the RSC was shown to play a central role in spatial memory and navigation (Vann et al. 2009). Similar observations were made in animal experiments using rodents (Vann et al. 2009). In rodents, the medial limbic cortex has been subdivided into anterior cingulate, posterior cingulate, and retrosplenial regions (Zilles et al. 1985). Interestingly, the RSC cortex represents one of the largest cortical areas in the rat. Similar to the primate RSC, the rat RSC can be subdivided into a dysgranular (area 30) and granular (area 29) regions (Van Groen and Wyss 1990a). The RSC is considered as an intermediate cortex since it displays a transitional pattern of lamination compared with the 6-layered neocortex and the 3-layered archicortex (Van Groen and Wyss 1990a).

Although much has been learned about the adult structure and functions of the CGC and RSC, little is known about their development. Early studies in the rat using injections of [3H]thymidine described the embryonic morphogenesis of the medial limbic cortex (Bayer 1990a, 1990b). Similar to neocortex, the medial limbic region develops in an "inside-out" fashion; infragranular deep cells are generated earlier than supragranular superficial cells (Bayer 1990a, 1990b). Interestingly, these studies also revealed important differences in the neurogenic pattern between the neocortex and the limbic areas. While in the neocortex, neurons in medial regions are generated later than those in more lateral subdivision, in the limbic cortex more ventral medial parts contain the older, early-generated neurons. It appears therefore that the medial limbic cortex is not a continuation of the adjacent somatic neocortex, at least in terms of ontogenetic pattern. More recent studies have characterized the postnatal dendritic development of supragranular pyramidal cells in the RSC (Ichinohe, Yoshihara, et al. 2003; Miro-Bernie et al. 2006; Miyashita et al. 2010) as well as the temporal pattern of formation of callosal connections from deep layer neurons (see review in Fame et al. 2011). While together these studies provide a wealth of information on the general pattern of neurogenesis and developmental events with regard to dendritic and axonal growth, the precise timing and dynamics of migration and positioning of neuronal precursors in the medial limbic cortex remain unexplored. This question is particularly relevant not only for the coordinated events that regulate cortical network formation under normal conditions but also for understanding neurodevelopmental disorders. The CGC and RSC have been implicated in major psychiatric pathologies such as schizophrenia (Bluhm et al. 2009) that are associated with developmental disturbances. In addition, neurons in these cortices appear particularly vulnerable to perinatal adverse effects of stress (Rivarola and Suarez 2009) and hypoxia (Li et al. 1998).

Here we focused on the sequential events of migration and positioning of late-born pyramidal cells in the medial limbic

cortex. These neurons are critically important for intracortical network formation, and their migration is of particular interest since they have a relatively long and complicated trajectory through pools of previously established neurons. We have started our investigations by using in vivo injections of lentivectors coding fluorescent proteins to label ventricular/subventricular zones (VZ/SVZ) precursors in newborn rat pups. Our results revealed a prominent pool of postmitotic cortical glutamatergic precursors localized in the dm corner of the VZ/SVZ underlying the medial limbic cortex. We demonstrate that these cells exit the SVZ and migrate radially toward the layer II (LII) during the first postnatal week, constituting the last-formed pyramidal subpopulation of the medial limbic cortex. In the retrosplenial granular cortex (RSGC), the majority of these cells gave rise to well-described dendritic-bundling cells. These studies extend previous work and provide the first insight into the pattern and dynamics of late-born neuron migration into the medial limbic cortex.

Materials and Methods

Animals

The experimental procedures described here were conducted in accordance with the Swiss laws, previously approved by the Geneva Cantonal Veterinary Authority. In these studies, embryonic day (E) 0 was established as the day of vaginal plug and the day of birth is designated as postnatal day (P) 0. Wistar rats were provided by Charles River Laboratories. The generation and characterization of transgenic mice expressing green fluorescent protein (GFP) under the control of the GAD65 promoter were described elsewhere (Lopez-Bendito et al. 2004).

Nomenclature

The RSC is divided into 2 parts, retrosplenial dysgranular cortex (or agranular) and RSGC (Wyss and Sripanidkulchai 1984; Van Groen and Wyss 1990a, 1990b, 2003) Along the rostrocaudal axis, the RSC is subdivided into the rostral RSC, which is found before the splenium of the corpus callosum, and the caudal RSC, which is found at the level of the splenium of the corpus callosum (Vogt and Peters 1981). Cortical layers were defined using Nissl stain, histochemical, and immunohistochemical markers. Layer I (LI) was further divided into 3 sublayers: 1a, 1b, and 1c (Vogt et al. 1981; Van Groen and Wyss 1990a; Wyss et al. 1990).

In Vivo Lentivector Injections

Wistar pups at P0/P1 were anesthetized with Isofluran (Foren 2%) in a mixture of 30% O_2 and 70% of air and placed in a stereotaxic apparatus. A short skin midline incision was carried out on the head at the level of the bregma, and a burr hole was placed at the surface of the skull on the right hemisphere with a thin needle (0.3 × 13 mm). The coordinates from the bregma were as follows: 0.8 mm anterior, 0.5 mm lateral, for medial injections, and from 0 to 0.8 mm anterior, from 1 to 1.5 mm lateral, for lateral injections. One microliter of concentrated lentivector suspension was injected with a Hamilton syringe (a 10-μl Hamilton (Reno, NV) syringe with a 28-gauge needle) at a depth of 1.3 mm from the surface of the brain. The same surgical protocol was applied in P0 GAD65 transgenic mice. These experiments were performed in a level-2 animal facility (AKA AniP2).

Design and Production of Lentivectors

The lentivectors used in this study (pFUGW or RIX) contain the ubiquitin promoter controlling the expression of GFP (pFUGW) (http://tronolab.epfl.ch/) or tdTomato (Tom) (RIX) (Shaner et al. 2004). Ubiquitin is ubiquitous and active in neural cells. The lentiviral vectors were produced, concentrated, and titrated (titers ranging from 10^8 to 10^9 transducing units [TU]/mL) according to standard protocols (Salmon and Trono 2006). Details on procedures can be obtained at http://medweb2.unige.ch/salmon/lentilab/protocols.html). Prior to in vivo injections, all lentivectors were tested in vitro in SVZ-derived neural progenitor cell (NPC) cultures as previously described (Dayer et al. 2007). Transduction was done at day in vitro 3 using doses ranging from 5×10^4 to 5×10^5 TU per 50 000–75 000 cells in a 35-mm culture dish, and no toxic effects on NPCs were detected (Dayer et al. 2007).

Tissue Processing and Immunohistochemistry

For post hoc in vivo studies, rats were anesthetized by pentobarbital and sacrificed by intracardial perfusion of 0.9% saline followed by 4% paraformaldehyde (PFA). Brains were postfixed overnight in 4% PFA at 4 °C. For rats younger than P2, the brains were directly fixed in 4% PFA without perfusion. For histological analyses of the postnatal VZ/SVZ, brains were embedded in paraffin, serially cut at 10 μm thickness on a coronal or horizontal plane with a Leica microtome (Germany), and stained with cresyl violet. Immunostaining of cryostat or vibratome sections was performed as described previously (Dayer et al. 2007). Briefly, sections were incubated with a primary antibody diluted in phosphate-buffered saline (PBS)/0.5% bovine serum albumin/0.3% Triton X-100, incubated with the appropriate secondary antibodies, and mounted on microscope glass slides. A list of primary and secondary antibodies used is available in Supplementary materials. For bromodeoxyuridine (BrdU) immunolabeling, 60- to 80-μm floating sections were first acid treated with 2 N HCl for 60 min at 37 °C, then carefully washed in PBS, and stained as above to detect Tom/GFP expression and to detect BrdU with a monoclonal rat anti-BrdU (1:250, Lucerna Chem AG).

Birthdating Experiments

To identify the birthdates of postnatally migrating cells, pregnant rats received a single intraperitoneal (IP) dose of 50 mg/kg body weight of BrdU at a given day of gestation (E17–E21). To assess the postnatal generation, rat pups received 3 daily IP injections of 20 mg/kg body weight from P0 to P3. Injections of lentivectors at P0 were carried out as described above. Animals were killed at P15, and the proportion of Tom-labeled BrdU-positive cells in LII was examined in the rostral RSC on the total amount of Tom-labeled cells.

Cortical Slice Preparation and Time-Lapse Imaging

For slice cultures, Tom-lentivector–injected pups were sacrificed by rapid decapitation at P1–P3; brains were removed, and coronal/sagittal slices (200–300 μm thick) were cut on a Vibratome (Vibratome Company, St Louis) and then placed on porous nitrocellulose inserts (Millicell-CM, Millipore). Slices were cultured in a 35-mm culture dish containing 2 mL of serum-complemented medium at 37 °C with 5% CO_2. After 6 h, serum-complemented medium was washed and replaced by serum-free medium. Images of brain slices were acquired with a digital camera (Retiga EX; Qimaging, Burnaby, Canada) connected to a ×0.6 lens (Nikon) linked to a fluorescent microscope (Eclipse TE2000-U; Nikon Corp., Zurich, Switzerland) equipped with a chamber maintained at 37 °C with 5% CO_2. Time-lapse recordings were acquired on slices containing the rostral RSC with Openlab software for a time window of 30 h (1 image each 10 min).

Image and Data Analysis

For analyses on post hoc tissue, immunostained slices were examined with a Nikon Eclipse TE2000-U microscope using Nikon objectives and photographed with a digital camera (Retiga EX; Qimaging) controlled by the Openlab software (version 3.1.2; Improvision, Coventry, UK). For analyses at high-power magnifications, Zeiss LSM 510 and LSM 510 Meta confocal microscopes with a Plan-Neofluar ×40/1.3 Oil objective were used. Image processing and cell quantification were performed with the program LSM Image Browser version 4,2,0,121. For analyses of migrating cells on radial glial fibers, images were processed by IMARIS 4.3 software (Bitplane). Distribution of lentivector-labeled migrating cells along the migratory way at P2, P4, and P7 was quantified by using Adobe Photoshop (Adobe Systems Incorporated, San Jose, CA) on epifluorescent images taken with a ×10 objective.

For quantification of immunostained cells (multiple fluorochromes) in the VZ/SVZ/white matter (WM)/LII and for quantification of cell distribution on the migratory path, analyses were performed at the level of the rostral RSC and cell counts were carried out on at least 3 coronal sections per brain from a minimum of 2 independent experiments for a given immunostaining and for a given time point. Except when indicated, results are expressed as mean ± standard error of the mean (SEM) and are presented as percentage on the total amount of counted lentivector-labeled cells in a given region (VZ/SVZ, WM, LII, and migratory path); n = number of analyzed brains.

For video time-lapse analyses, single-cell tracking was performed with MetaMorph Software (Molecular Devices, version 7.4). Results for speed and persistence are presented as percentage (mean ± SEM) from 4 independent experiments, and n = number of analyzed cells. The persistence rate was calculated as the ratio of the most direct distance the cell progressed along the total path length. Statistical Student's t-test (bilateral) was performed on population samples, and statistical significance was defined at $P < 0.05$ (*) and $P < 0.01$ (**). For measures of the length of cell processes, results are shown as absolute values (mean ± SEM) from at least 3 independent experiments, and n = number of slices. For categorization of migrating cells in the WM, results are presented as percentage (mean ± SEM) from 4 independent experiments, and n = number of slices.

Details of experimental manipulations and analyses can be found in Supplementary material.

Results

Postnatal Radial Migration into the Medial Limbic Cortex

In order to identify cortex-directed cell movement from the VZ/SVZ to the medial limbic cortex during the early postnatal period, lentiviral vectors carrying either the GFP or the red fluorescent Tom protein under an ubiquitous promoter were injected stereotactically into the right lateral ventricle of P0/P1 rat pups. This approach allowed to label a wide range of cells in the VZ/SVZ, including nonproliferative cells. Two to 3 days after the injection, we studied the distribution of fluorescent cells in sagittal and coronal brain sections. When we used standard intraventricular injections, we observed a large number of labeled cells in the wall of ipsilateral ventricular system as well as radial glial fibers spanning the cortex (Supplementary Fig. 1). Moreover, a massive labeling was observed in the lateral SVZ, the rostral migratory stream, and granular layer of the olfactory bulb in sagittal slices (Supplementary Fig. 1). However, in general, and in agreement with previous reports (Levison and Goldman 1993; Zerlin et al. 1995; Kakita and Goldman 1999), no labeled neuroblasts appeared migrating radially out of the dorsal VZ/SVZ to the cortex. Therefore, we changed the coordinates of injections to specifically target the dm aspect of the lateral ventricle lying below the medial limbic cortex. We found that, under these conditions (0.5 mm lateral to the bregma) (Fig. 1*A*), the labeling of the dmVZ/SVZ was much more pronounced, and a substantial number of labeled, radially oriented cells seemed to migrate out of the dmVZ/SVZ into the medial limbic cortex (Fig. 1*B–F*). These cells could be seen remote from the injection site, more rostrally (CGC) and more caudally (RSC), and resembled migrating neuroblasts. Remarkably, in a number of cases, labeled migrating cells even occurred in the contralateral hemisphere (Fig. 1*D–F*). This latter correlated with a strong bilateral labeling of the dmVZ/SVZ. Importantly, labeled migrating cells in the cortex were detected only when the lentivectors were delivered between P0 and P1 but not in the following days. Identical results were obtained after medial lentivector injections in P0/P1 mice (not shown). Taken together, these data suggest that the dm subdomain of the VZ/SVZ in neonatal rodents is the source of a neuronal population, which postnatally migrates into the medial limbic cortex.

A Premigratory Pyramidal Precursor Pool in the Neonatal dmVZ/SVZ

To investigate the precise origin of radially migrating cells into the medial limbic cortex, we explored the dmVZ/SVZ on Nissl-stained coronal sections between P0 and P7. We observed that a large pool of immature, irregularly oriented, and darkly stained cells was located in the dmVZ/SVZ at P0 (red arrowhead, Fig. 2*A,B*). This cell pool significantly diminished by P3 (Fig. 2*A*), suggesting that a transient population of premigratory and immature cells homes in the dmVZ/SVZ at birth. We also observed that the dmVZ/SVZ is located in close anatomical relationship with the cavum septum pellucidum (CSP) (Fig. 2*B*). The CSP is a transitory structure during the early postnatal development that is located at the corticoseptal boundary (Dart 1925; Tseng et al. 1983). Its extremities extend dorsally and rostrocaudally and sometimes appear as lacunae (black arrowheads, Fig. 2*B* right panel). Because the dmVZ/SVZ extends quite far from the lateral ventricle toward the midline, it occupies the lateral sector of the CSP (red arrowheads, Fig. 2*B*).

A closer inspection of fluorescent cells in the vicinity of CSP revealed labeled cells not only in the dmVZ/SVZ but also in neighboring midline cell populations. As illustrated in Figure 2*C*, these cell groups include the glial wedge (red arrowheads) located at the frontier between the lateral ventricle and the CSP, the sling (yellow arrowheads), lining the lateral septal nuclei on the floor of the CSP, and the midline glial zipper (white arrowhead), which is positioned at the midline below the corpus callosum (see review in Lindwall et al. 2007). Quantitative data confirmed that medial injections labeling these midline cell populations were systematically associated with fluorescent radially migrating cells in the medial limbic cortex (81.9%, 50 out of a total of 61 brains analyzed). From these observations, we inferred that by performing medial injections reaching the frontier between the lateral ventricle and the CSP, we were able to produce widespread lentivector diffusion in the CSP allowing an efficient labeling of the surrounding regions including the dmVZ/SVZ (uni- or bilaterally) (schematic drawing, Fig. 2*D*).

To characterize the phenotype of postnatally migrating cells, we performed immunocytochemistry for transcription factors that are expressed in different types of neural precursor cells during development. When we analyzed the P2 dmVZ/SVZ, we found that about 37% of GFP+ cells expressed paired box 6 (Pax6) immunoreactivity (Fig. 2*F,G*), a homeodomain transcription factor that is mainly expressed by radial glia and different subtypes of progenitors (see review in Hevner et al. 2006). Immunocytochemistry for Tbr2, a transcription factor expressed in intermediate progenitors (basal precursors) of the pyramidal cell lineage (Kowalczyk et al. 2009), revealed that 33% of GFP+ cells in the VZ/SVZ expressed Tbr2 (Fig. 2*E,F*, Supplementary Fig. 2A). More than 50% of GFP+ cells in the VZ/SVZ were immunoreactive for NeuroD (Fig. 2*F*, Supplementary Fig. 2A), a marker of late intermediate progenitors committed to glutamatergic neurons (Hevner et al. 2006). We also examined the expression of Satb2, a transcription factor

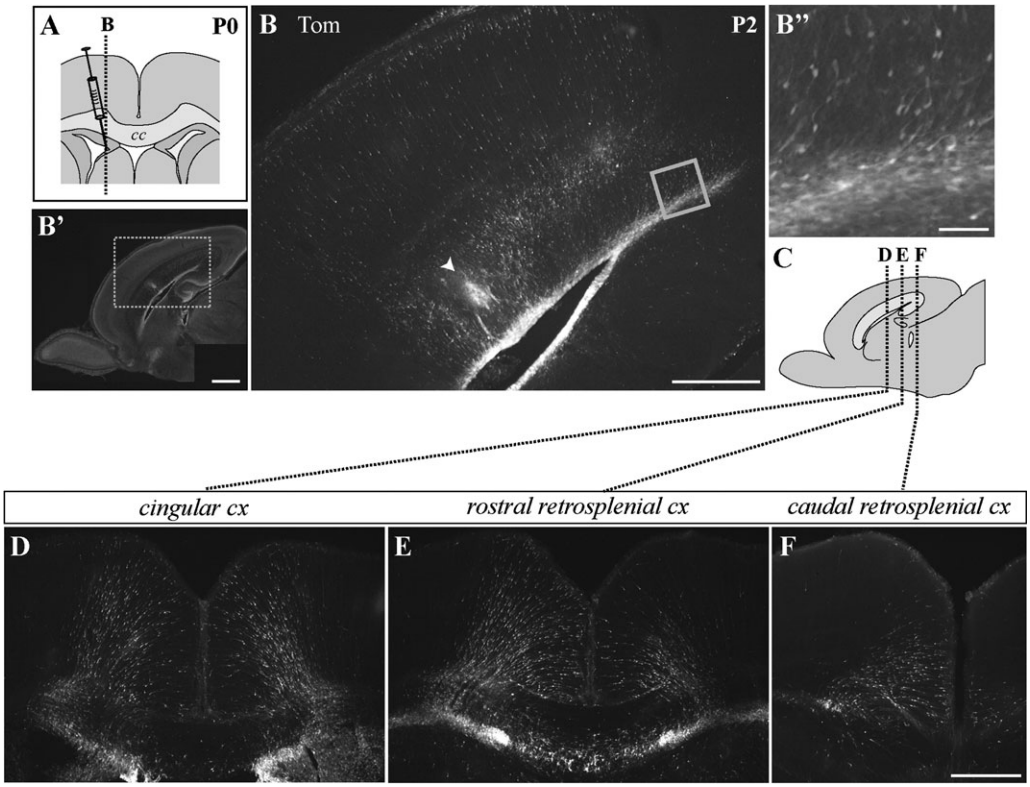

Figure 1. Intraventricular medial lentivector injections at P0 reveal a large pool of labeled radially oriented cells in the medial limbic cortex 2 days after injection. (*A*) Schematic drawing of a coronal brain section depicting the site of medial lentivector injection at P0. (*B*, *D–F*) Epifluorescent images of sagittal (*B*) and coronal (*D–F*) vibratome sections illustrating the pattern of fluorescence 2 days after a medial injection of Tom-lentivector. Images reveal a massive labeling of the dmVZ/SVZ and a large number of labeled cells spanning the medial cortex outside the injection track (arrowhead in *B*); (*B*) is a higher magnification of the boxed area in (*B′*), which shows the same section by Hoechst nuclear staining. (*B″*) Higher magnification of the boxed area in (*B*) evidencing columns of radially oriented cells starting from the SVZ and oriented to the cortex. Sagittal plane of (*B–B″*) is indicated by dotted line in (*A*). (*C*) Schematic drawing of a sagittal section indicates rostrocaudal levels of coronal images in (*D–F*). cc, Corpus callosum; cx, cortex. Scale bar = 1000 μm for (*B′*), 500 μm for (*B*, *D–F*), 50 μm for (*B″*).

predominantly expressed in cortical pyramidal neurons with callosal projections (Britanova et al. 2005). We found that a subset, about 20%, of GFP+ cells in the dmVZ/SVZ were Satb2+ (Fig. 2*E*,*F*). Interestingly, Satb2+ cells were distributed in the outer zone of dmSVZ showing minimal overlapping with the Tbr2+ cell population (Fig. 2*E*). We also observed that about 10% of GFP-labeled cells within the VZ/SVZ expressed the chondroitin sulfate proteoglycan NG2 (Fig. 2*F*), a marker for oligodendrocyte precursors (see review in Karram et al. 2005), and 19% of the GFP-labeled cells expressed immunoreactivity for S100β (Fig. 2*F*), a marker for astrocytes and ependymal cells (Raponi et al. 2007).

When we investigated the phenotype of GFP+ cells migrating through the WM overlying the dmVZ/SVZ, we found that most GFP-labeled cells exiting from the SVZ had lost Tbr2 and Pax6 immunoreactivity (Fig. 2*E–G*, Supplementary Fig. 2A), whereas many cells were seen positive for NeuroD (Fig. 2*F*,*H*, supplementary Fig. 2A). Most importantly, we found that strong immunostaining for Satb2 was present in about 77% of GFP+ cells traversing the WM (Fig. 2*E*,*F*,*H*). A similar percentage of GFP-labeled cells (79%) (Fig. 2*F*,*I*, Supplementary Fig. 2B) expressed doublecortin (DCX) immunoreactivity, a common marker for migrating γ-aminobutyric acidergic (GABAergic) and glutamatergic neurons (Gleeson et al. 1999). Finally, about 6% of GFP-labeled cells in the WM were positive for S100β and 20% for NG2 (Fig. 2*F*). These data indicate that the vast majority of fluorescent migrating cells have a neuronal phenotype. Moreover, the fact that approximately the same percentage of migrating GFP+ cells expressed DCX and Satb2 strongly suggested that postnatally migrating cells from the SVZ were glutamatergic cells. To confirm this hypothesis, we took advantage of GAD65-GFP transgenic mice, in which GABAergic interneurons express GFP fluorescence. As shown in Supplementary Figure 3A–D, GFP fluorescence in those mice did not cover the most medial aspect of VZ/SVZ labeled by Tom fluorescence after medial Tom-lentivector injections; moreover, the Tom+ migratory cell population did rarely overlap with the GFP+ population of GABAergic interneurons ($4.9 \pm 0.4\%$, $n = 3$).

Together, these observations revealed that a significant pool of premigratory, glutamatergic precursor cells is located in the early postnatal dmSVZ and that this region represents a reservoir for a subset of Satb2-expressing glutamatergic neurons, which migrate early after birth.

Postnatally Migrating Cells toward the Medial Limbic Cortex Display a Pyramidal Phenotype and Position in LII

Labeled migrating cells toward the medial limbic cortex were arranged radially in paralleled arrays (Fig. 3*A*) and often lined up forming continuous cell chains (Fig. 3*D*,*E*). Most of the fluorescent cells presented the structural characteristics of radially migrating pyramidal cells (Fig. 3*A–C*) including the bipolar-shaped, elongated soma with a constriction in the center, the unbranched leading process, and the thin trailing process (Rakic 1972; O'Rourke et al. 1992; Hatanaka and Murakami 2002).

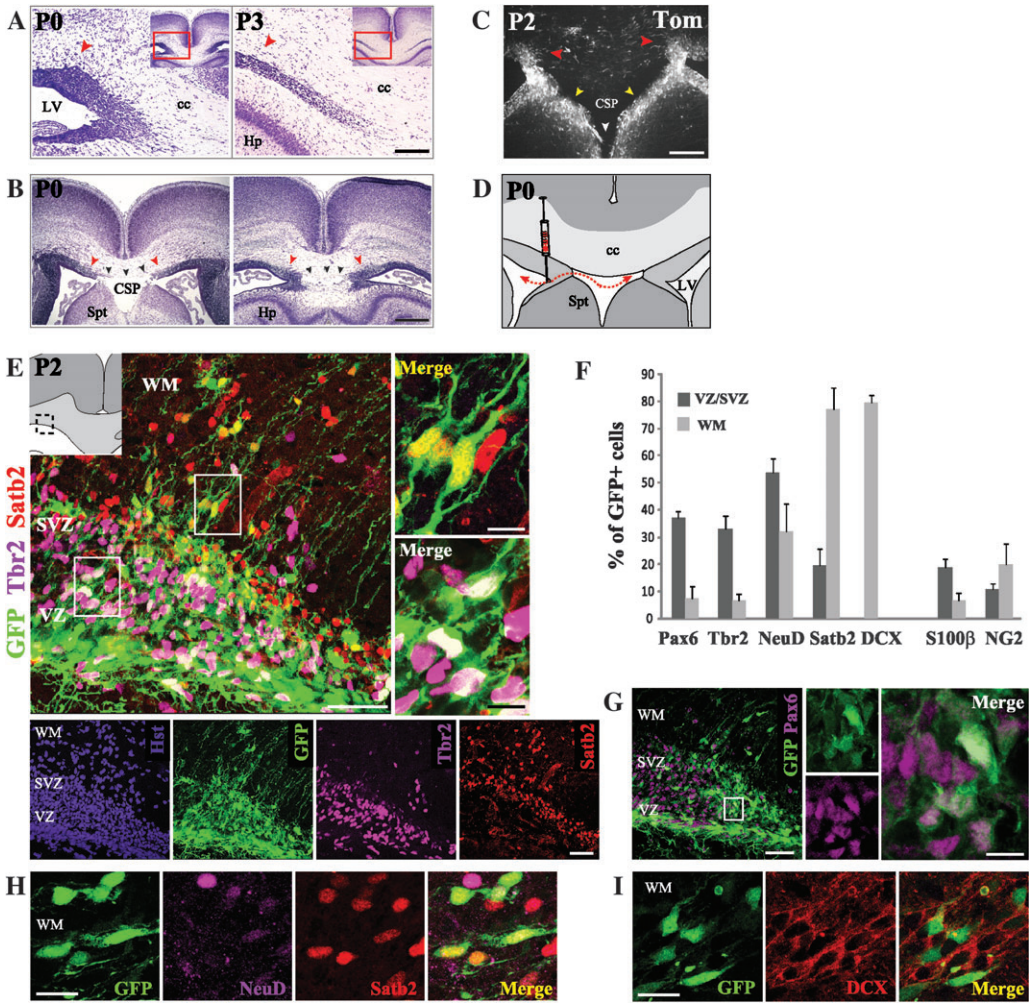

Figure 2. Medial lentivector injections reach the cavum septum pellucidum and label a glutamatergic cell pool in the dmVZ/SVZ. (A) Nissl-stained coronal sections showing that the size of the caudal dmVZ/SVZ (red arrowheads) decreases from P0 (left) to P3 (right). Images are higher magnifications of red squares in the insets. (*B*) Nissl-stained horizontal sections showing the dmSVZ/VZ (red arrowheads) at P0 and its location in relationship to the CSP (black arrowheads) from dorsal (left panel) to ventral (right panel) levels. (*C*) Epifluorescent image from a coronal section illustrating pattern of lentivector labeling in the CSP at P2. Additional labeled cell populations include the glial wedge (red arrowheads), the sling (yellow arrowheads), and the midline glial zipper (white arrowhead). (*D*) Schematic drawing illustrating that medial lentivector injections target the dm corner of lateral ventricle allowing lentivector diffusion (red dotted lines) in the CSP and labeling of the dmVZ/SVZ bilaterally. (*E*, *G–I*) Confocal images showing immunostaining of GFP-labeled cells (green) for different phenotypic markers in the dmVZ/SVZ and WM at P2. Image location for (*E*, *G*) is indicated by the square in the top left inset. (*E*) Merge image of Tbr2 (purple) and Satb2 (red) immunostaining. Single-channel images of the same section are shown on the bottom and compared with Hoechst staining (blue). Higher magnifications of the 2 boxed areas are shown on the right and illustrate colocalization of Satb2 and GFP (upper panel, yellow) in migrating cells and of Tbr2 and GFP (bottom panel, white) in VZ/SVZ progenitors. (*F*) Quantification of the colocalization of GFP labeling with different phenotypic markers in the VZ/SVZ (gray) and WM (light gray). Bars represent mean ± SEM of at least 2 independent experiments. (*G*) Pax6 (purple) immunoreactivity in the dmVZ/SVZ and WM; right panels are higher magnifications of the boxed area in the left panel and show colocalization of Pax6 and GFP (white) in VZ/SVZ progenitors. (*H*) Expression of NeuD (purple, *H*), Satb2 (red, *H*), and (*I*) DCX (red) in GFP+ migrating cells in the WM. Note that most of them are Satb2+ (yellow, *H*) and DCX+ (*I*) and that some Satb+/GFP+ coexpress NeuD (light yellow, *H*). cc, Corpus callosum; Spt, septum; LV, lateral ventricle; Hp, hippocampus; NeuD, NeuroD. Scale bar = 500 μm for (*B*), 200 μm for (*A*, *C*), 50 μm for (*E*, *G*), 10 μm for high-power images in (*E*, *G*), and 20 μm for (*H*, *I*).

In line with these observations, we found that the orientation of labeled migrating cells always parallels those of nestin+ radial glial fibers and that precursor cells appear to migrate in close apposition with radially oriented glial fibers (Fig. 3*A*,*D*,*E*).

While many fluorescent migrating cells were scattered in different layers during the first 3 postnatal days, at P4, the majority of cells had reached the marginal zone (Fig. 3*F*) and at P7 almost all cells were accumulated in LII (Fig. 3*G*,*I*). Quantitative analyses confirmed that postnatal cortex-directed migration takes place during the first 5–7 days (Fig. 3*H*). At P2, roughly 60% of fluorescent cells were distributed over LV–VI, while less than 40% were located in the cortical plate. By P7, about 98% of the total population of pyramidal-like cells were in LII (Fig. 3*H*). It is important to note that from P5, an increasing number of fluorescent cells with multipolar glial morphology were also detected in LV–VI. The appearance of these cells is consistent with the notion of postnatal gliogenesis from the SVZ (Kakita and Goldman 1999). Cells with glial morphology were not included in cell counts.

We also observed that at P7, labeled cells positioned in LII (Fig. 3*I*) appeared as a homogenous neuronal population: they were pyramidal shaped and they showed a thin beaded axon-like process extending toward the inner cortex and a thick dendrite-like process invading LI with multiple branching (Fig. 3*I*). Moreover, about 90% (88.70 ± 1.25%, $n = 4$) of them were positive for the pyramidal cell marker Satb2 (Fig. 3*I*), whereas

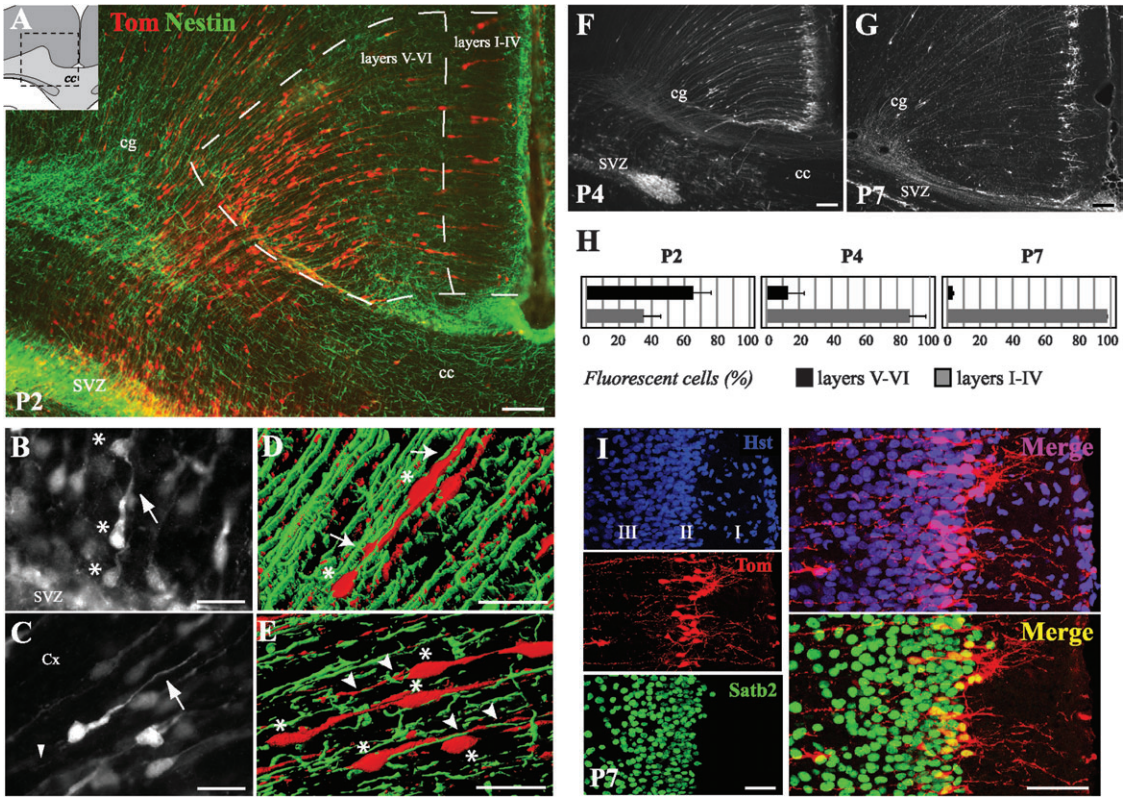

Figure 3. Lentivector-labeled migrating cells are associated with the radial glial fibers and gradually populate LII. (*A*) Epifluorescent image of a P2 coronal section showing that Tom-labeled migrating cells (red) are regularly aligned and follow the general orientation of radial glial fibers (nestin immunostaining, green). The image is an enlargement of the boxed region in the top left inset. (*B*, *C*) Higher power images illustrating the general morphology of Tom-labeled cells traversing the WM (*B*) and cortex (Cx), (*C*). In the late phase of migration through the Cx, the leading process is longer (arrows) and the trailing process is more visible (arrowheads in *C*) than in the early phase through the WM. (*D*, *E*) The 3D Z-stack reconstruction of confocal images illustrating that Tom+ migrating cells (red) are closely associated with Nestin+ radial glial fibers (green) (arrows in *D*) and that their leading processes can be found coiled around them (arrowheads in *E*) and/or held on the trailing process/cell body of the preceding cell (asterisks in *D*, *E*). Note that labeled cells often seem to attach one to each other, thus forming chains of migrating cells (asterisks in *B*, *D*, *E*). (*F*, *G*) Pattern of Tom fluorescence from animals sacrificed, respectively, 4 days (*F*) and 7 days (*G*) after lentivector injection; at P4, most of lentivector-labeled cells have reached their final destination close to pial surface, whereas migration seems completed at P7. Image location is the same than (*A*). (*H*) Graphs indicating the percentage of labeled cells in cortical LV/VI (black) and LI–IV (gray) at P2, P4, and P7. The medial cortical region crossed by labeled migrating cells has been divided in 2 sectors according to the main anatomical landmarks present: LV/VI and LI–IV (white dashed line in *A*). Bars represent mean ± SEM of at least 2 independent experiments. (*I*) Single-channel (left panels) and double merge (right panels) confocal images at the level of LII showing that Tom-labeled cells (red) position in LII (blue, Hoechst nuclear staining) and express the Satb2 marker (green). cc, Corpus callosum; cg, cingulum. Romanic numbers indicate layers. Scale bar = 100 μm for (*A*, *F*, *G*), 50 μm for (*I*), and 20 μm for (*B*–*E*).

only 5% expressed GAD67 (4.74 ± 0.82%, $n = 3$) immunoreactivity, a marker for GABAergic interneurons. Satb2+ cells in layer II but not during migration were also lightly positive for Tbr1 (Supplementary Fig. 3E), an additional transcription factor which is known to be expressed downstream of Pax6 in glutamatergic neurogenesis (Hevner et al. 2001).

Postnatally Migrating Cells Are Generated at Embryonic Ages

To investigate the time window in which postnatally migrating neurons are generated, rats were exposed to BrdU at E17, E18, E19, E20, E21, or from P0 to P3. These animals were subjected to P0 medial lentivector injections and killed at P15. Post hoc immunohistochemistry on coronal brain sections allowed evaluating the colocalizations of BrdU (green) and Tom (red) immunolabeling in neurons deployed in LII of the rostral RSGC (Fig. 4*A*,*B*). Our analysis indicated that less than 15% of lentivector-labeled cells were born after E20, whereas about 70% (70.75%) of them arise from cell division between 18th and 19th days of gestation (Fig. 4*B*). We also found that after BrdU labeling at E18/E19, BrdU-immunostained cells accumulate in the dmVZ/SVZ at P0 and decrease at P3 (Fig. 4*C*). Thus, pyramidal precursors, which migrate out of the VZ/SVZ postnatally, are already postmitotic at P0.

Dynamics of Cell Migration into the Medial Limbic Cortex

Next, we analyzed the migratory behavior of lentivector-labeled postnatally migrating cells. For this purpose, animals received a medial injection of Tom-lentivector at P0 and time-lapse imaging was carried out for more than 24 h in fresh cortical slice preparation at the level of the RSC from P1 to P3 animals. We focused on the rostral regions of the RSC and distinguished between 2 phases of migration. During the first phase of migration ("i", Fig. 5*A*), radially oriented fluorescent cells detach from SVZ and migrate toward the dorsal edge of the cingulum through the WM ("i", Supplementary movie 1). Within the WM, the great majority of migrating cells adopted an elongated shape with a unipolar or bipolar morphology (blue arrows, Supplementary movie 2). Cells displayed a leading process (arrowheads, Fig. 5*B*–*E*) in a dorsal direction and a less visible trailing process (arrows, Fig. 5*B*,*D*). The average length of the leading process was 54.78 ± 1.19 μm ($n = 3$, 35 cells). Time-lapse analysis indicated that cells moved by locomotion in a discontinuous, saltatory manner ("i", Fig. 5*I*) with a mean speed of 17 μm/h ($n = 168$,

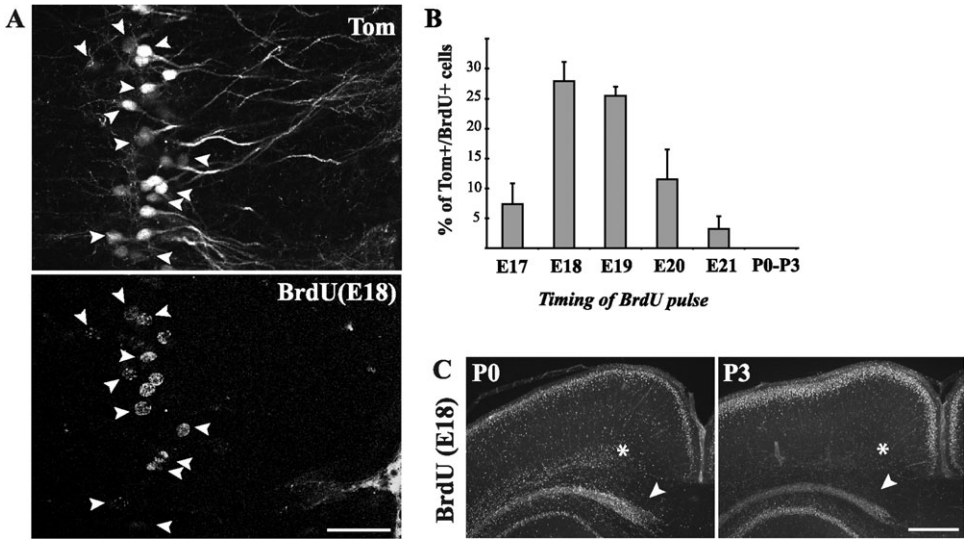

Figure 4. Lentivector-labeled cells populating LII of the RSC are generated between E17 and E21. (*A*) Single channel confocal images showing Tomato (top panel) and BrdU (lower panel) immunoreactivity in LII of the RSC from coronal sections of P15 rats, which received BrdU injection at E18 and Tom-lentivector at P0. White arrowheads in both images indicate double-labeled cells revealing that many LII Tom+ cells are born at E18. (*B*) Graph indicating that the majority of lentivector-labeled cells located in LII are generated between E18 and E19, whereas virtually no labeled cells are generated postnatally. Bars represent mean ± standard error. (*C*) Epifluorescent images showing BrdU immunostaining on caudal coronal brain slices of 2 animals exposed to BrdU on E18 and sacrificed, respectively, at P0 (left panel) and P3 (right panel). At P0, the dmVZ/SVZ (arrowheads) and the cingular region (asterisk) have a strong BrdU immunoreactivity, whereas few BrdU+ cells have reached the superficial cortical layers; in the same regions, at P3, the BrdU immunoreactivity in the VZ/SVZ and cingular region is decreased and a large amount of BrdU+ cells appear in the superficial cortical layers. Scale bar = 50 μm for (*A*) and 500 μm for (*C*).

6 slices; Fig. 5*J*). Interestingly, at least 20% (20.96 ± 5.56%, $n = 6$, 168 cells) of the tracked cell population extended a leading process with branches. In these cases, the soma moved toward the branching point of the leading process and then cells retracted branches and moved in the direction of the remaining branch (Fig. 5*E*; red arrows, Supplementary movie 2). This process of alternating formation and retraction of branches was accompanied by frequent changes in the direction of movement. Nevertheless, as a population, cells moved toward the dorsal edge of the cingulum (Fig. 5*F*).

During the second phase of migration ("ii", Fig. 5*A*), labeled cells leave the WM and migrate toward the pial surface of the cortex. Similar to the migration during the first phase, the movement of the cells in the gray matter (GM) was saltatory ("ii", Fig. 5*I*; Supplementary movie 3) and the mean speed approached 17 μm/h ($n = 85$, 4 slices; Fig. 5*J*). However, in the GM, cells showed less frequent directional changes (Fig. 5*H*), resulting in a significantly higher (4.3%) persistence ratio compared with that calculated for the first migratory phase (Fig. 5*J*). Cells also became progressively more elongated (Fig. 5*G*) compared with those migrating within the WM; the average length of the leading process reached roughly 100 μm (102.6 ± 1.51 μm, $n = 4$, 35 cells), and cells often developed a prominent trailing process (23.72 ± 7.89 μm, $n = 4$, 19 cells) (arrows at 100 min, Fig. 5*G*). This later could even reach the length of 300 μm (arrows at 590 min, Fig. 5*G*; Supplementary movie 4) and grow in the opposite direction of the cell body, thus becoming a prospective axon (Supplementary movie 4). On the contrary, the leading process maintained a relatively constant length and remained unbranched (arrowheads, Fig. 5*G*; Supplementary movie 4). As the cells approached the pial surface, their leading process became thicker and progressively shorter, the soma stopped migrating, and the cells changed their bipolar form to a multipolar morphology (image not shown).

These results demonstrate that postnatally migrating cells present typical dynamic characteristics of radially migrating pyramidal cells described previously. Moreover, they display important morphological and behavioral changes as they progressed through the WM and the GM.

Postnatally Migrating Cells Differentiate into Dendritic Bundles Forming Pyramidal Neurons in the RSGC

To investigate the final fate of postnatally migrating cells, morphology of labeled cells in LII was analyzed at progressive postnatal time points. We first observed that labeled LII extended paralleled axons that reached the cingular region and curved to cross the midline through the upper corpus callosum (Fig. 6*A*,*E*). Most interestingly, we found that in the RSGC, the apical dendrite and the secondary branches of neighboring cells converged together in LIb–c forming typical dendritic bundles (DB) (Fig. 6*A*–*E*) intercalated with empty regions, the interbundle spaces. The dendritic tree of these cells spread out in the outer part of LI (1a), so that the extremities of neighboring dendritic branches joined each other. Characteristically, a group of LII pyramidal cells giving rise to a DB displayed an hourglass shape. We did not observe similar arrangement of neurons in neighboring cortex (Fig. 6*A*). This pattern was similar to that reported by others (Wyss et al. 1990; Ichinohe and Rockland 2002; Ichinohe et al. 2003b) and described as honeycomb-like mosaic. By confocal imaging (Fig. 6*I*) and the microtubule-associated protein 2 (MAP2), and the AMPA (alpha-amino-3-hydroxy-5-methyl-4- isoxazole-propionic acid)-type glutamate receptor subunits GluR2/3 immunohistochemistry (Supplementary Fig. 4), we confirmed the development of this DB configuration over time. Moreover, immunocytochemical characterization of labeled cells in the adult rostral RSGC (Supplementary Fig. 5) showed that the large majority of LII

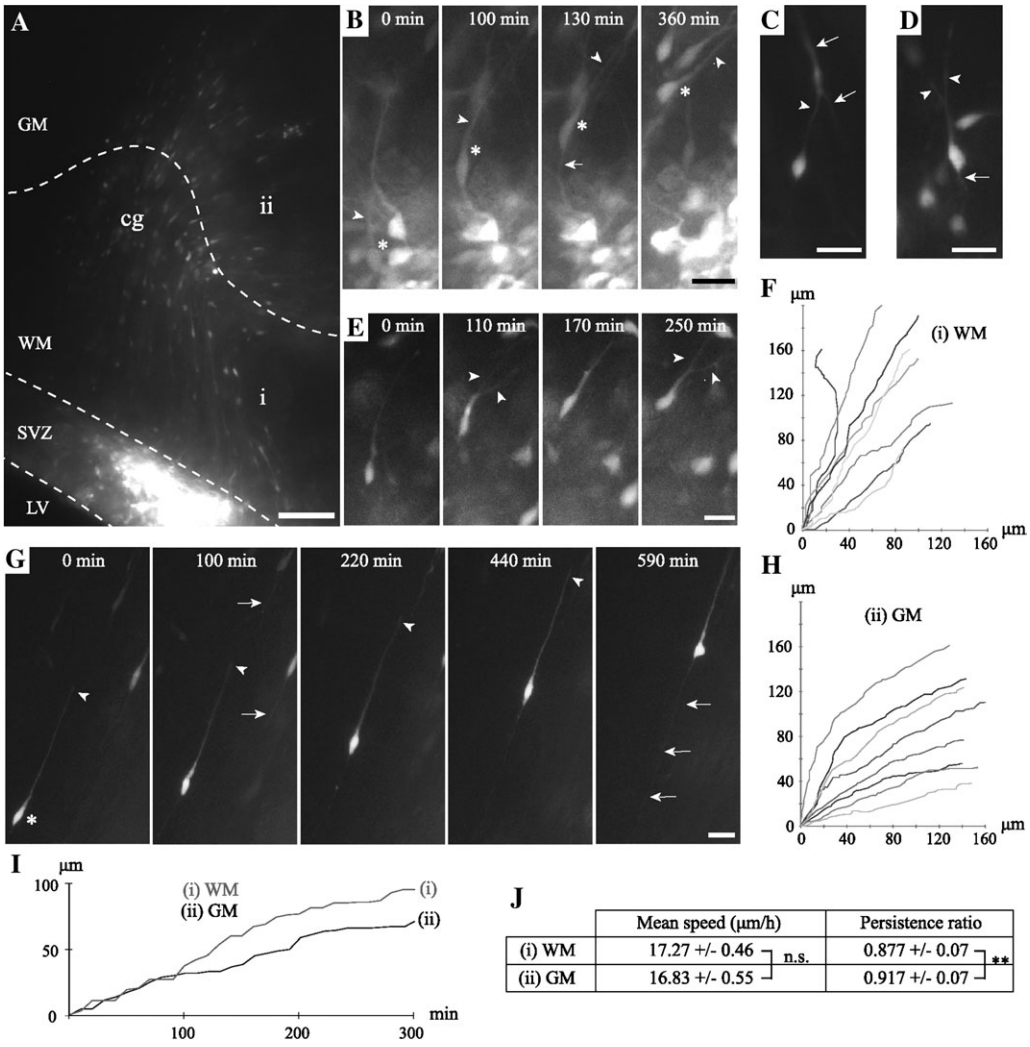

Figure 5. Dynamics of postnatal cell migration from the dmVZ/SVZ into the medial limbic cortex. (*A*) Epifluorescent image of a P2 brain slice after P0 injection of Tom-lentivector showing the migratory path of labeled cells from the dmVZ/SVZ, through the WM and the GM. Cell migration occurring in WM and GM was recorded continuously by time-lapse frame grapping (10 min of interval) from day in vitro (DIV) 0 to DIV1, and the migration tracks were, respectively, plotted in a scatter diagram (*F*, *H*). (*B*) Time-lapse sequence showing a labeled cell (asterisk) exiting the SVZ and displaying an unbranched leading process (arrowhead). (*C*) Labeled cell with an unbranched leading process (arrowhead) makes contact with a radial glial process (arrows). (*D*) Representative cell with branched leading process (arrowheads) and a short trailing process (arrow). (*E*) Time-lapse sequence showing unbranched and branched (arrowheads) configurations of a labeled migrating cell. (*F*) Migration tracks of labeled cells during migration through the WM. The starting point for each cell is in the intersection between the *X*- and *Y*-axes (0;0). (*G*) Time-lapse sequence of labeled cells (asterisk) migrating in the GM. Note that migrating cells display a long leading process (arrowhead) as well as a trailing process (arrows). (*H*) Migration tracks of labeled cells during GM migration. (*I*) Diagram representing the distance traveled by 2 individual labeled cells during WM and GM migration. In both phases, cells migrate in a saltatory fashion, alternating between migratory and static phases, resulting in a stair-like track. (*J*) Table showing the average speed and persistence of migrating cells during WM and GM migration. Results are shown as mean ± SEM. Bilateral Student's *T*-test was used for statistical analysis (n.s., $P = 0.5567$; **, $P = 0.00081$). Abbreviations as in previous figures. Scale bar = 100 µm for (*A*) and 20 µm for (*B*, *C*, *D*, *E*, *G*).

lentivector-labeled cell population (75.11 ± 2.54%, $n = 4$; Supplementary Fig. 5B,C) was immunolabeled for GluR2/3 and that the half of this population in addition expressed calbindin (44.11 ± 0.17%, $n = 3$; Supplementary Fig. 5B,C). Both of these markers have been reported to characterize LII pyramidal cells forming DB (Ichinohe, Fujiyama, et al. 2003).

All together, these observations indicate that postnatally migrating progenitor cells in the RSGC give rise to a specific cell type: LII pyramidal neurons known to form DB in LI.

Discussion

Here, we identified and characterized delayed migratory events that govern the positioning of the late-born pyramidal neurons in the medial limbic cortex. We observed that a large pool of postmitotic precursor cells is located in the early postnatal dmSVZ representing a reservoir for Satb2-expressing glutamatergic neurons (see Fig. 7). Cohorts of cells exit from this premigratory pool and migrate into the RSC and CGC during the first postnatal week. This migration is robust and guided by the radial glial scaffold. Time-lapse imaging demonstrates that this population of postnatally migrating pyramidal cells displays important morphological and behavioral changes as cells traverse the WM and subsequently the cortical GM. In the granular RSC, the large majority of these cells give rise to a specific cell type: Satb2+, LII pyramidal cells with typical DB in LI.

Origin of Postnatally Migrating Cells

Recent studies using retroviral labeling of SVZ progenitors in vivo aimed to directly observe cortex-directed migration in

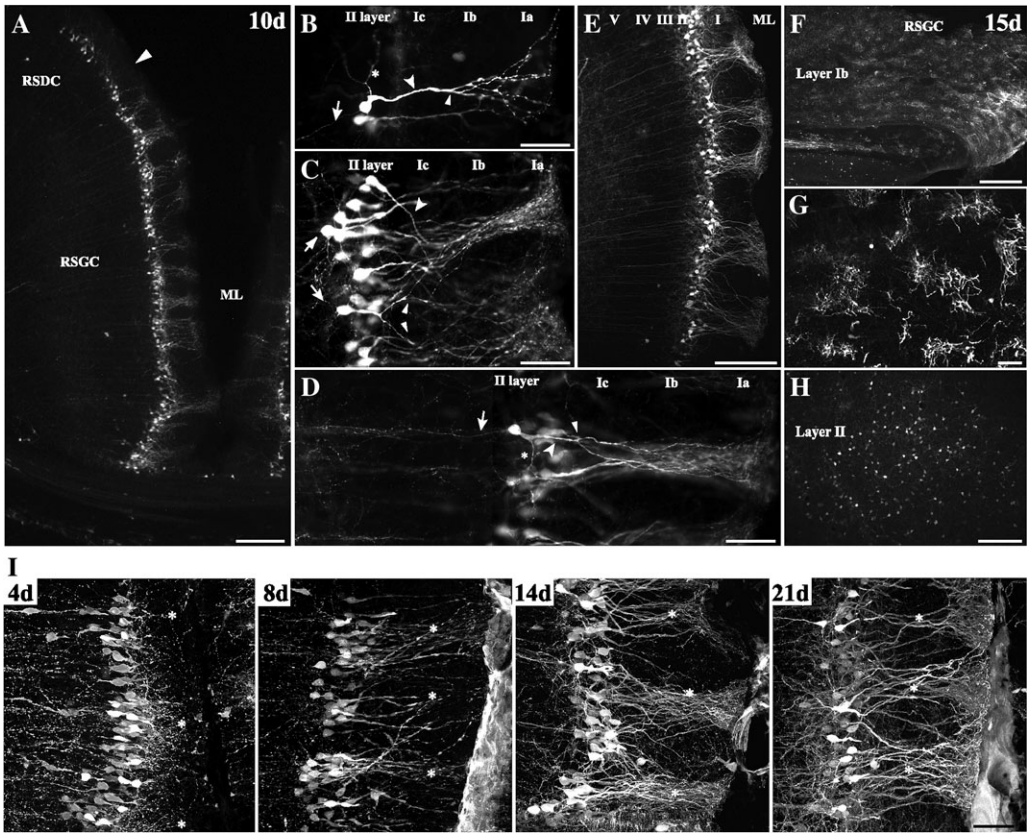

Figure 6. Lentivector-labeled cells form characteristic DB in LII of the RSGC. (*A–H*) Epifluorescent images of lentivector fluorescence in brain sections at the level of rostral RSGC 10 days (*A*) and 15 days (*B–H*) after medial lentivector injection. (*A*) Coronal brain section illustrating that dendrites of labeled cells form DB in LI of RSGC cortex (arrowhead indicate limit between subcortical regions). Note that these dendritic structures are not present in the retrosplenial dysgranular cortex. Note also fluorescent axons of LII cells descending toward the cingular regions and traveling through the upper part of the corpus callosum. (*B–E*) Higher magnifications of LI-II from P15 coronal brain sections showing cell morphologies of LII cells and DB shapes in LI. Labeled cells in LII present thin basal dendrites located in LII (asterisks in *B*, *D*) and a thick single apical dendrite (large arrowheads in *B–D*) bifurcating in LIb (small arrowhead in *B*) or in LIc (small arrowhead in *D*) and arborizing extensively in the outer part of LI. (*B–D*) Dendritic arbors of multiple neighboring LII cells join together at the level of LIb and overlap in LIa–b to form DB of various size and shape. (*C–E*) Apical dendritic branches extend straight to LI (large arrowheads in *B*, *D*) or angle to reach lateral DB (large arrowhead in *C*) or even bifurcate and reach 2 neighboring DB by different second-order branches (small arrowheads in *C*). The axonal processes of LII cells (*B–D*, arrows) travel on parallel rails directed to the inner part of RSGC (*E*). (*F–H*) Sagittal brain sections through LIb (*F*, *G*) and LII (*H*) illustrating, respectively, the pattern and morphology of DB in LIb (*F*, *G*) and the distribution of LII cell bodies (*H*) in LII. Note the honeycomb-like mosaic formed by DB in LIb (*F*, *G*). (*I*) Z-stack reconstruction of confocal images showing the progressive formation of DB (asterisks) from 4 to 21 days after medial lentivector injection. ML, midline. Scale bar = 200 μm for (*A*, *E*, *H*), 50 μm for (*B–D*, *G*, *I*), and 500 μm for (*F*).

newborn animals (Levison et al. 1993; Suzuki and Goldman 2003). The results obtained led to the general conclusion that cell migration from the SVZ during the early postnatal period is characterized by glial cell migration (Cayre et al. 2009). Two major differences distinguish the present investigation from these earlier studies. First, we used lentiviral labeling of SVZ that, in contrast to retroviral transduction, does not require mitotically active cells and thus labels dividing as well as nondividing cells. Second, we targeted lentivector at the dm corner of the lateral ventricle that was not investigated in earlier studies. We demonstrate that in order to visualize postnatally migrating neurons, lentiviral injections must reach the dm sector of the VZ/SVZ. This region is in close anatomical relationship with the CSP, a transitory structure which is present from E18 to P15 (Dart 1925; Tseng et al. 1983). It is very likely that pressure injection in the dm corner of the ventricle has generated small openings in the ventricular wall allowing the access for viral particles into this space. This hypothesis is consistent with our observation that medial injections frequently lead to ipsi- as well as contralateral labeling of migrating cells. Moreover, the CSP may allow for distributing lentivector particles in the rostrocaudal direction from the injection site, thus leading to labeling in regions situated more caudally. Finally, we systematically observed labeled cells in midline structures in relationship with the CSP, including the glial wedge and the glial sling (Shu et al. 2003). Thus, the CSP appears to play a pivotal role in distributing viral particles in the dmSVZ bilaterally following medially directed injections. The histological analysis confirmed that a large contingent of irregularly oriented, immature cells is accumulated in the dmVZ/SVZ in the vicinity of the CSP at P0. During the first postnatal week, we observed radially oriented cells exiting the dmSVZ and the size of the SVZ pool is considerably decreased by P3. It appears therefore that our lentivector-mediated labeling protocol at P0/P1 allows to visualize a pool of cells in the lateral CSP/dmSVZ that give rise to postnatally migrating pyramidal neurons.

Postnatally Migrating Cells Form a Homogenous Pyramidal Cell Population in LII of the Medial Limbic Cortex

Our results indicate that the vast majority of postnatally migrating cells from the dmSVZ integrate into the CGC and

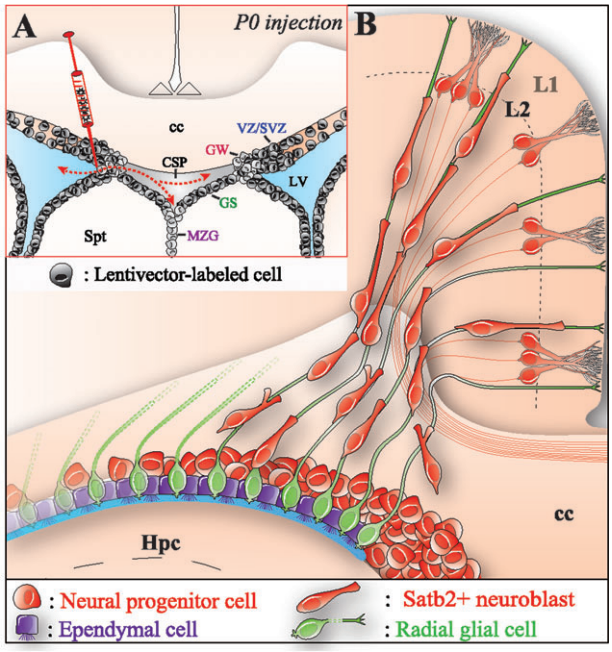

Figure 7. Early postnatal migration and development of a dmSVZ pyramidal cell population to the medial limbic cortex. (*A*) Schematic representation of a coronal section of P0 brain illustrating the site of medial lentivector injection and the pattern of lentivector particles dispersion in the CSP and lateral ventricles (LV) (red arrows) as well as the lentivector-labeled cell populations (black–gray cells). Strongly labeled cell populations include the dmVZ/SVZ, the glial sling (GS), the glial wedge (GW), and the midline zipper glia (MZG). (*B*) Schematic representation of the midline region at the level of the RSC. Migratory glutamatergic progenitors exit from the dmSVZ region during the 3 first postnatal days and follow curved radial glial paths. Labeled cells express Satb2 and settle in LII of the medial limbic cortex by the end of the first postnatal week. Satb2+ cells send transcallosal axons through the upper corpus callosum (cc) to the contralateral cortex. In the RSGC, they also form DB in LI. Abbreviations as in previous figures.

RSC. We found that while many fluorescent migrating precursors were scattered in different cortical layers during the first postnatal week, by P7, virtually all these cells were accumulated in LII and displayed a pyramidal morphology. Consistent with this observation, we demonstrate that more than 50% of labeled cells in the dmSVZ expressed markers for glutamatergic precursors such as Tbr2, NeuroD, and Satb2 (Britanova et al. 2005; Hevner et al. 2006). Satb2 is a DNA-binding protein known to be expressed in postmitotic pyramidal neurons with callosal projections (Britanova et al. 2005; Szemes et al. 2006; Alcamo et al. 2008). Knockout experiments in mice have demonstrated that Satb2 plays a crucial role in the specification of laminar cell-type identity and in development of callosal projections (Alcamo et al. 2008; Britanova et al. 2008). Strikingly, we found that about 80% of labeled cells were immunolabeled for Satb2 after exiting the SVZ, indicating that the majority of postnatally migrating precursors differentiate into the pyramidal neurons of LII with callosal projections. Our birthdating experiments demonstrate that virtually all postnatally migrating cells are generated between E17 and E21, indicating that the precursor pool in the SVZ is already postmitotic in newborns. These data well correlate with earlier studies demonstrating the course of neurogenesis in the medial limbic cortex following [3H]thymidin labeling of the germinal layer (Bayer 1990b). The presence of an important cohort of postmitotic precursor cells in the newborn SVZ is in agreement with previous observations, indicating that following the division of progenitor cells in the VZ cells accumulate in the basal part of the SVZ and could stay there for several days in rodents (Tabata et al. 2009). Our BrdU labeling experiments suggest that lentivector-labeled postnatally migrating precursors may stay up to 5 days (from E17 to P0) in the SVZ. The longer sojourn in the SVZ appears to be characteristic for late migrating pyramidal populations (Hicks and D'amato 1968; Bayer and Altman 1991; Ignacio et al. 1995; Tarabykin et al. 2001). It would be interesting to explore whether this relatively long stopover period in the SVZ is related to a putative synchronization process between thalamic afferent ingrowth and the migration/positioning of neurons as suggested by Bayer (1990b) and Altman and Bayer (2002). Noteworthy in this respect is that we found a subset of lentivector-labeled cells expressing Satb2 immunoreactivity within the outer layer of the early postnatal SVZ. Thus, the specification of postnatally migrating pyramidal precursors in terms of Satb2 expression seems to start within the SVZ during the transformation of precursors into locomotion cells. Satb2 messenger RNA expression has been reported in the upper part of embryonic SVZ at middle corticogenesis (Britanova et al. 2005; Britanova et al. 2006); however, it has not been found in this region at later stages, and Satb2 protein expression in premigratory cells of SVZ remained controversial (Britanova 2005; Alcamo et al. 2008). Although, knockout experiments in mice and downregulation of Satb2 expression have shown to impair pyramidal cell migration during corticogenesis (Britanova et al. 2008), the mechanisms of such effect remain unclear. Demonstrating Satb2 protein expression in the premigratory cell pool further highlights the potential role of Satb2 in cell migration.

Although the majority of cortical interneurons are arising from the medial ganglionic eminence (MGE) and reach the cortex after tangential migration (Wonders and Anderson 2006; Gelman and Marin 2010), the dorsal SVZ in mice may also be the source of precursors for calretinin-positive GABAergic interneurons that may be positioned in cortical layers after

radial migration (Inta et al. 2008; Vucurovic et al. 2010). Of particular interest in this respect is that in human and nonhuman primate, the outer subventricular proliferative zones also contribute to the generation of cortical interneurons at late phases of cortical development (Letinic et al. 2002; Petanjek et al. 2009). This population shows a significant expansion from rodents to primates, and it is considered as a primate-specific morphological feature (Jones 2009; Rakic et al. 2009). In this study, we found that less than 5% of the postnatally migrating neurons in LII displayed GABAergic phenotype. The precise origin of these cells, whether they arrive into the SVZ from the MGE or from the lateral/caudal ganglionic eminence, remains to be determined. Future studies should explore the relevance of this small pool of neurons for the postnatal development of rodent limbic circuits and whether this population shows a numerical expansion in the human and primates compared with rodents.

Radial Migration in the Early Postnatal Period

The postnatal migration of pyramidal precursors into supragranular layers is of particular interest since these cells have a relatively long and complicated trajectory through pools of previously established neurons. Indeed, labeled neuronal progenitors followed a curved path that corresponds to the path drawn by radial glial fibers between the dm neuroepithelium and the pial surface of midline cortex. We demonstrate that the principal migratory mode of late-generated pyramidal precursor cells in the medial cortex, just as in neocortical regions (Rakic 1972; Nadarajah et al. 2001; Tamamaki et al. 2001; Tabata and Nakajima 2003), is locomotion, characterized by the typical saltatory movement on the radial glial scaffold. We did not observe somal translocation that was described to occur during early corticogenesis (Miyata et al. 2001). The migration rate by locomotion that we calculated in this study (17 μm/h) was comparable with that observed by O'Rourke et al. (1992) (11 μm/h) but much slower than that reported by Nadarajah et al. (2001) (35 μm/h). This discrepancy may be due to the difference in experimental conditions in the slice preparations and the age of the tissue. We did not observe significant difference in migration speed in the WM compared with that we measured in the GM. In addition, we did not see multipolar migration of SVZ progenitors as has been described in the SVZ (Tabata and Nakajima 2003; Hatanaka et al. 2004; Ohshima et al. 2007; Tabata et al. 2009). However, an intriguing observation of the present study is that some of the radially migrating cells, especially in the WM, display movement that is referred in the literature as a distinct migratory mode: branched migration (Gupta et al. 2003; Nadarajah et al. 2003). In these cases, migrating cells that had an unbranched leading process at a certain time point of migration may extend new branches on the leading process. In view of the highly dynamic process of formation and retraction of small branches, cells with this type of movement have been considered as actively exploring their environment for guidance cues. This type of morphology was mainly described for interneurons migrating in the tangential plane (Valiente and Martini 2009) without being a prerogative of these cells (Ward et al. 2005; Lopez-Bendito et al. 2006). Among others, we have seen a number of putative interneurons in our slice preparations moving with this mode of migration especially in the tangential plane. Indeed, branching migration in cortical pyramidal cells has been rarely observed (Nadarajah et al. 2003; Elias et al. 2007) and rather associated with defects on cell contacts between migrating neurons and radial glial fibers (Gupta et al. 2003; Elias et al. 2007). However, we believe that our radially migrating cells with branched morphology are pyramidal precursors and not just radially oriented interneurons. First, while interneurons migrating by branching move with a relatively high speed (40 μm/h) (Valiente and Martini 2009), the average speed of radially moving branched cells was the same (about 17 μm/h) than those of unbranched radially migrating cells. Second, unlike interneurons, radially moving branched cells did not have prominent growth cones. It is important to emphasize here that branched migration occurred in a significant proportion of pyramidal cells migrating through the WM but not in the GM. This is consistent with the hypothesis that many of the pyramidal precursors after leaving the SVZ are still in an exploratory mode and might not yet establish firm adhesion with the radial scaffold. The conjecture of a more "unstable" migration in the WM received support from our observation that migration paths of individual cells in the WM were more "zigzagged" and cells appeared switching from one glial fiber to another. This phenomenon may be even more pronounced in the context of the medial limbic cortex where the radial glial path is particularly curved. In line with these observations, the calculated persistence of migration was significantly lower in the WM than that in the GM where cells migrated in a far more directed fashion. Importantly, our results of branched pyramidal precursors using video imaging were confirmed by the presence of branched bipolar cells on the glial scaffold in our post hoc materials.

The Final Fate of Postnatally Migrating Pyramidal Precursors

The rodent RSC is a simplified "limbic" cortex that is positioned within the transition zone between the 3-layered hippocampal archicortex and the 6-layered neocortex (Vogt and Laureys 2005). It has reciprocal connections with neighboring hippocampal, parahippocampal, and neocortical regions and plays a central role in spatial learning and memory (Gabriel and Sparenborg 1987; Cooper et al. 2001; Vann and Aggleton 2002). A distinctive feature of this cortical region is the presence of DB formed by apical dendrites of LII pyramidal cells (Wyss et al. 1990; Ichinohe and Rockland 2002; Ichinohe et al. 2008; Miyashita et al. 2010). The precise function of these neurons remains to be elucidated. While these structures have been documented in great detail, little is known about the origin and the migration pattern of DB forming cells during development. We describe here that postnatally migrating cells transform into pyramidal cells with characteristic DB. Retrosplenial DB are composed of glutamatergic neurons and GABA/parvalbumine-positive inhibitory neurons (Wyss et al. 1990; Ichinohe and Rockland 2002). In line with previous reports (Ichinohe et al. 2003b; Miro-Bernie et al. 2006), our immunohistochemical analyses demonstrate that the majority of lentivector-labeled cells expressed the GluR2/3 subunit of the AMPA receptor. From this population, nearly 50% of the cells (45.41%) were also weakly immunoreactive for calbindin (Supplementary Fig. 3C), a marker already used to describe dendritic-bundling cells in rat visual cortex (Ichinohe et al. 2003a). Because calbindin has been shown to be transitory in some type of cells (Celio 1990; Alcantara et al. 1993; Alcantara and Ferrer 1995), the differences

in the expression of these markers between LII cells may alternatively reflect the presence of variability in the functional state of these cells. Our results describing the expression pattern of MAP2 and GluR2/3 in the early and late (P4–P30) development of the DB formation confirm earlier studies (Ichinohe et al. 2003b). The fact that the large majority of migrating cells and neurons settled in LII express Satb2 is consistent with the notion that these cells are transcallosal-projecting neurons (Wyss et al. 1990).

Conclusion

In conclusion, using lentivector-mediated fluorescent labeling and video time-lapse analysis, we describe a pool of pyramidal cell precursors in the dmSVZ that migrate into the medial limbic cortex during the early postnatal period. We show that in the RSGC, the majority of these cells give rise to LII DB forming cells. To our knowledge, this is the first study that describes the migratory dynamics and positioning of a specific cell type in the postnatal limbic cortex. This new model may permit to follow the development of an identified cell type over several developmental stages from the premigratory cell pool through the radially migrating neuroblast stage to the positioning of LII pyramidal cells with the progressive elaboration of DB, spine formation, and axonal growth. Future studies could focus on the impact of afferent systems and environmental factors including adverse effects on these developmental events and to evaluate how alterations of these processes contribute to neurodevelopmental disorders. This question is particularly relevant to the human CGC and RSC that has been implicated in psychiatric disorders with putative neurodevelopmental basis.

Funding

Swiss National Foundation (31003-130781/1); Special Program University Medicine (33CM30-124101); Von Meissner and Novartis foundations to J.Z.K.

Supplementary Material

Supplementary material can be found at: http://www.cercor.oxfordjournals.org/.

Notes

We wish to thank Beatrice King, Sylvie Chliate, and Cynthia Saadi for technical assistance. *Conflict of Interest*: none declared.

References

Alcamo EA, Chirivella L, Dautzenberg M, Dobreva G, Farinas I, Grosschedl R, Mcconnell SK. 2008. Satb2 regulates callosal projection neuron identity in the developing cerebral cortex. Neuron. 57:364–377.

Alcantara S, Ferrer I. 1995. Postnatal development of calbindin-D28k immunoreactivity in the cerebral cortex of the cat. Anat Embryol (Berl). 192:369–384.

Alcantara S, Ferrer I, Soriano E. 1993. Postnatal development of parvalbumin and calbindin D28K immunoreactivities in the cerebral cortex of the rat. Anat Embryol (Berl). 188:63–73.

Altman J, Bayer SA. 2002. Regional differences in the stratified transitional field and the honeycomb matrix of the developing human cerebral cortex. J Neurocytol. 31:613–632.

Bayer SA. 1990a. Development of the lateral and medial limbic cortices in the rat in relation to cortical phylogeny. Exp Neurol. 107:118–131.

Bayer SA. 1990b. Neurogenetic patterns in the medial limbic cortex of the rat related to anatomical connections with the thalamus and striatum. Exp Neurol. 107:132–142.

Bayer SA, Altman J. 1991. Neocortical development. New York: Raven Press.

Bluhm RL, Miller J, Lanius RA, Osuch EA, Boksman K, Neufeld RW, Theberge J, Schaefer B, Williamson PC. 2009. Retrosplenial cortex connectivity in schizophrenia. Psychiatry Res. 174:17–23.

Britanova O, Akopov S, Lukyanov S, Gruss P, Tarabykin V. 2005. Novel transcription factor Satb2 interacts with matrix attachment region DNA elements in a tissue-specific manner and demonstrates cell-type-dependent expression in the developing mouse CNS. Eur J Neurosci. 21:658–668.

Britanova O, Alifragis P, Junek S, Jones K, Gruss P, Tarabykin V. 2006. A novel mode of tangential migration of cortical projection neurons. Dev Biol. 298:299–311.

Britanova O, De Juan Romero C, Cheung A, Kwan KY, Schwark M, Gyorgy A, Vogel T, Akopov S, Mitkovski M, Agoston D, et al. 2008. Satb2 is a postmitotic determinant for upper-layer neuron specification in the neocortex. Neuron. 57:378–392.

Cayre M, Canoll P, Goldman JE. 2009. Cell migration in the normal and pathological postnatal mammalian brain. Prog Neurobiol. 88:41–63.

Celio MR. 1990. Calbindin D-28k and parvalbumin in the rat nervous system. Neuroscience. 35:375–475.

Cooper BG, Manka TF, Mizumori SJ. 2001. Finding your way in the dark: the retrosplenial cortex contributes to spatial memory and navigation without visual cues. Behav Neurosci. 115:1012–1028.

Dart RA. 1925. The genesis of the cavum septi pellucidi. J Anat. 59:369–378.

Dayer AG, Jenny B, Sauvain MO, Potter G, Salmon P, Zgraggen E, Kanemitsu M, Gascon E, Sizonenko S, Trono D, et al. 2007. Expression of FGF-2 in neural progenitor cells enhances their potential for cellular brain repair in the rodent cortex. Brain. 130:2962–2976.

Elias LA, Wang DD, Kriegstein AR. 2007. Gap junction adhesion is necessary for radial migration in the neocortex. Nature. 448:901–907.

Fame RM, Macdonald JL, Macklis JD. 2011. Development, specification, and diversity of callosal projection neurons. Trends Neurosci. 34:41–50.

Gabriel M, Sparenborg S. 1987. Posterior cingulate cortical lesions eliminate learning-related unit activity in the anterior cingulate cortex. Brain Res. 409:151–157.

Gelman DM, Marin O. 2010. Generation of interneuron diversity in the mouse cerebral cortex. Eur J Neurosci. 31:2136–2141.

Gleeson JG, Lin PT, Flanagan LA, Walsh CA. 1999. Doublecortin is a microtubule-associated protein and is expressed widely by migrating neurons. Neuron. 23:257–271.

Gupta A, Sanada K, Miyamoto DT, Rovelstad S, Nadarajah B, Pearlman AL, Brunstrom J, Tsai LH. 2003. Layering defect in p35 deficiency is linked to improper neuronal-glial interaction in radial migration. Nat Neurosci. 6:1284–1291.

Hatanaka Y, Hisanaga S, Heizmann CW, Murakami F. 2004. Distinct migratory behavior of early- and late-born neurons derived from the cortical ventricular zone. J Comp Neurol. 479:1–14.

Hatanaka Y, Murakami F. 2002. In vitro analysis of the origin, migratory behavior, and maturation of cortical pyramidal cells. J Comp Neurol. 454:1–14.

Hevner RF, Hodge RD, Daza RA, Englund C. 2006. Transcription factors in glutamatergic neurogenesis: conserved programs in neocortex, cerebellum, and adult hippocampus. Neurosci Res. 55:223–233.

Hevner RF, Shi L, Justice N, Hsueh Y, Sheng M, Smiga S, Bulfone A, Goffinet AM, Campagnoni AT, Rubenstein JL. 2001. Tbr1 regulates differentiation of the preplate and layer 6. Neuron. 29:353–366.

Hicks SP, D'amato CJ. 1968. Cell migrations to the isocortex in the rat. Anat Rec. 160:619–634.

Ichinohe N, Fujiyama F, Kaneko T, Rockland KS. 2003. Honeycomb-like mosaic at the border of layers 1 and 2 in the cerebral cortex. J Neurosci. 23:1372–1382.

Ichinohe N, Knight A, Ogawa M, Ohshima T, Mikoshiba K, Yoshihara Y, Terashima T, Rockland KS. 2008. Unusual patch-matrix organization in the retrosplenial cortex of the reeler mouse and Shaking rat Kawasaki. Cereb Cortex. 18:1125–1138.

Ichinohe N, Rockland KS. 2002. Parvalbumin positive dendrites co-localize with apical dendritic bundles in rat retrosplenial cortex. Neuroreport. 13:757–761.

Ichinohe N, Yoshihara Y, Hashikawa T, Rockland KS. 2003. Developmental study of dendritic bundles in layer 1 of the rat granular retrosplenial cortex with special reference to a cell adhesion molecule, OCAM. Eur J Neurosci. 18:1764–1774.

Ignacio MP, Kimm EJ, Kageyama GH, Yu J, Robertson RT. 1995. Postnatal migration of neurons and formation of laminae in rat cerebral cortex. Anat Embryol (Berl). 191:89–100.

Inta D, Alfonso J, Von Engelhardt J, Kreuzberg MM, Meyer AH, Van Hooft JA, Monyer H. 2008. Neurogenesis and widespread forebrain migration of distinct GABAergic neurons from the postnatal subventricular zone. Proc Natl Acad Sci U S A. 105:20994–20999.

Jones EG. 2009. The origins of cortical interneurons: mouse versus monkey and human. Cereb Cortex. 19:1953–1956.

Kakita A, Goldman JE. 1999. Patterns and dynamics of SVZ cell migration in the postnatal forebrain: monitoring living progenitors in slice preparations. Neuron. 23:461–472.

Karram K, Chatterjee N, Trotter J. 2005. NG2-expressing cells in the nervous system: role of the proteoglycan in migration and glial-neuron interaction. J Anat. 207:735–744.

Kowalczyk T, Pontious A, Englund C, Daza RA, Bedogni F, Hodge R, Attardo A, Bell C, Huttner WB, Hevner RF. 2009. Intermediate neuronal progenitors (basal progenitors) produce pyramidal-projection neurons for all layers of cerebral cortex. Cereb Cortex. 19:2439–2450.

Letinic K, Zoncu R, Rakic P. 2002. Origin of GABAergic neurons in the human neocortex. Nature. 417:645–649.

Levison SW, Chuang C, Abramson BJ, Goldman JE. 1993. The migrational patterns and developmental fates of glial precursors in the rat subventricular zone are temporally regulated. Development. 119:611–622.

Levison SW, Goldman JE. 1993. Both oligodendrocytes and astrocytes develop from progenitors in the subventricular zone of postnatal rat forebrain. Neuron. 10:201–212.

Li YB, Kaur C, Ling EA. 1998. Neuronal degeneration and microglial reaction in the fetal and postnatal rat brain after transient maternal hypoxia. Neurosci Res. 32:137–148.

Lindwall C, Fothergill T, Richards LJ. 2007. Commissure formation in the mammalian forebrain. Curr Opin Neurobiol. 17:3–14.

Lopez-Bendito G, Cautinat A, Sanchez JA, Bielle F, Flames N, Garratt AN, Talmage DA, Role LW, Charnay P, Marin O, et al. 2006. Tangential neuronal migration controls axon guidance: a role for neuregulin-1 in thalamocortical axon navigation. Cell. 125:127–142.

Lopez-Bendito G, Sturgess K, Erdelyi F, Szabo G, Molnar Z, Paulsen O. 2004. Preferential origin and layer destination of GAD65-GFP cortical interneurons. Cereb Cortex. 14:1122–1133.

Miro-Bernie N, Ichinohe N, Perez-Clausell J, Rockland KS. 2006. Zinc-rich transient vertical modules in the rat retrosplenial cortex during postnatal development. Neuroscience. 138:523–535.

Miyashita T, Wintzer M, Kurotani T, Konishi T, Ichinohe N, Rockland KS. 2010. Neurotrophin-3 is involved in the formation of apical dendritic bundles in cortical layer 2 of the rat. Cereb Cortex. 20:229–240.

Miyata T, Kawaguchi A, Okano H, Ogawa M. 2001. Asymmetric inheritance of radial glial fibers by cortical neurons. Neuron. 31:727–741.

Nadarajah B, Alifragis P, Wong RO, Parnavelas JG. 2003. Neuronal migration in the developing cerebral cortex: observations based on real-time imaging. Cereb Cortex. 13:607–611.

Nadarajah B, Brunstrom JE, Grutzendler J, Wong RO, Pearlman AL. 2001. Two modes of radial migration in early development of the cerebral cortex. Nat Neurosci. 4:143–150.

O'Rourke NA, Dailey ME, Smith SJ, Mcconnell SK. 1992. Diverse migratory pathways in the developing cerebral cortex. Science. 258:299–302.

Ohshima T, Hirasawa M, Tabata H, Mutoh T, Adachi T, Suzuki H, Saruta K, Iwasato T, Itohara S, Hashimoto M, et al. 2007. Cdk5 is required for multipolar-to-bipolar transition during radial neuronal migration and proper dendrite development of pyramidal neurons in the cerebral cortex. Development. 134:2273–2282.

Petanjek Z, Kostovic I, Esclapez M. 2009. Primate-specific origins and migration of cortical GABAergic neurons. Front Neuroanat. 3:26.

Rakic P. 1972. Mode of cell migration to the superficial layers of fetal monkey neocortex. J Comp Neurol. 145:61–83.

Rakic S, Yanagawa Y, Obata K, Faux C, Parnavelas JG, Nikolic M. 2009. Cortical interneurons require p35/Cdk5 for their migration and laminar organization. Cereb Cortex. 19:1857–1869.

Raponi E, Agenes F, Delphin C, Assard N, Baudier J, Legraverend C, Deloulme JC. 2007. S100B expression defines a state in which GFAP-expressing cells lose their neural stem cell potential and acquire a more mature developmental stage. Glia. 55:165–177.

Rivarola MA, Suarez MM. 2009. Early maternal separation and chronic variable stress in adulthood changes the neural activity and the expression of glucocorticoid receptor in limbic structures. Int J Dev Neurosci. 27:567–574.

Salmon P, Trono D. 2006. Production and titration of lentiviral vectors. Curr Protoc Neurosci. Chapter 4:4.21.

Shaner NC, Campbell RE, Steinbach PA, Giepmans BN, Palmer AE, Tsien RY. 2004. Improved monomeric red, orange and yellow fluorescent proteins derived from Discosoma sp. red fluorescent protein. Nat Biotechnol. 22:1567–1572.

Shu T, Puche AC, Richards LJ. 2003. Development of midline glial populations at the corticoseptal boundary. J Neurobiol. 57:81–94.

Suzuki SO, Goldman JE. 2003. Multiple cell populations in the early postnatal subventricular zone take distinct migratory pathways: a dynamic study of glial and neuronal progenitor migration. J Neurosci. 23:4240–4250.

Szemes M, Gyorgy A, Paweletz C, Dobi A, Agoston DV. 2006. Isolation and characterization of SATB2, a novel AT-rich DNA binding protein expressed in development- and cell-specific manner in the rat brain. Neurochem Res. 31:237–246.

Tabata H, Kanatani S, Nakajima K. 2009. Differences of migratory behavior between direct progeny of apical progenitors and basal progenitors in the developing cerebral cortex. Cereb Cortex. 19:2092–2105.

Tabata H, Nakajima K. 2003. Multipolar migration: the third mode of radial neuronal migration in the developing cerebral cortex. J Neurosci. 23:9996–10001.

Tamamaki N, Nakamura K, Okamoto K, Kaneko T. 2001. Radial glia is a progenitor of neocortical neurons in the developing cerebral cortex. Neurosci Res. 41:51–60.

Tarabykin V, Stoykova A, Usman N, Gruss P. 2001. Cortical upper layer neurons derive from the subventricular zone as indicated by Svet1 gene expression. Development. 128:1983–1993.

Tseng CY, Ling EA, Wong WC. 1983. Scanning electron microscopy of amoeboid microglial cells in the transient cavum septum pellucidum in pre- and postnatal rats. J Anat. 136:251–263.

Valiente M, Martini FJ. 2009. Migration of cortical interneurons relies on branched leading process dynamics. Cell Adh Migr. 3: 278–280.

Van Groen T, Wyss JM. 1990a. Connections of the retrosplenial granular a cortex in the rat. J Comp Neurol. 300:593–606.

Van Groen T, Wyss JM. 1990b. The postsubicular cortex in the rat: characterization of the fourth region of the subicular cortex and its connections. Brain Res. 529:165–177.

Van Groen T, Wyss JM. 2003. Connections of the retrosplenial granular b cortex in the rat. J Comp Neurol. 463:249–263.

Vann SD, Aggleton JP. 2002. Extensive cytotoxic lesions of the rat retrosplenial cortex reveal consistent deficits on tasks that tax allocentric spatial memory. Behav Neurosci. 116:85–94.

Vann SD, Aggleton JP, Maguire EA. 2009. What does the retrosplenial cortex do? Nat Rev Neurosci. 10:792–802.

Vogt BA. 2005. Pain and emotion interactions in subregions of the cingulate gyrus. Nat Rev Neurosci. 6:533–544.

Vogt BA, Laureys S. 2005. Posterior cingulate, precuneal and retrosplenial cortices: cytology and components of the neural network correlates of consciousness. Prog Brain Res. 150:205–217.
Vogt BA, Peters A. 1981. Form and distribution of neurons in rat cingulate cortex: areas 32, 24, and 29.. J Comp Neurol. 195: 603–625.
Vogt BA, Rosene DL, Peters A. 1981. Synaptic termination of thalamic and callosal afferents in cingulate cortex of the rat. J Comp Neurol. 201:265–283.
Vucurovic K, Gallopin T, Ferezou I, Rancillac A, Chameau P, Van Hooft JA, Geoffroy H, Monyer H, Rossier J, Vitalis T. 2010. Serotonin 3A receptor subtype as an early and protracted marker of cortical interneuron subpopulations. Cereb Cortex. 20:2333–2347.
Ward ME, Jiang H, Rao Y. 2005. Regulated formation and selection of neuronal processes underlie directional guidance of neuronal migration. Mol Cell Neurosci. 30:378–387.
Wonders CP, Anderson SA. 2006. The origin and specification of cortical interneurons. Nat Rev Neurosci. 7:687–696.
Wyss JM, Sripanidkulchai K. 1984. The topography of the mesencephalic and pontine projections from the cingulate cortex of the rat. Brain Res. 293:1–15.
Wyss JM, Van Groen T, Sripanidkulchai K. 1990. Dendritic bundling in layer I of granular retrosplenial cortex: intracellular labeling and selectivity of innervation. J Comp Neurol. 295:33–42.
Zerlin M, Levison SW, Goldman JE. 1995. Early patterns of migration, morphogenesis, and intermediate filament expression of subventricular zone cells in the postnatal rat forebrain. J Neurosci. 15:7238–7249.
Zilles K, Schleicher A, Glaser T, Traber J, Rath M. 1985. The ontogenetic development of serotonin (5-HT1) receptors in various cortical regions of the rat brain. Anat Embryol (Berl). 172:255–264.